J. Submicrosc. Cytol., 19 (2), 209-227, 1987

Prelesional events in atherogenesis. Changes induced by hypercholesterolemia in the cell surface chemistry of arterial endothelium and blood monocytes, in rabbit

N. GHINEA, M. LEABU, M. HASU, V. MURESAN, J. COLCEAG and N. SIMIONESCU

Institute of Cellular Biology and Pathology, Bucharest 79691, Romania

SUMMARY - We investigated the modifications that diet-induced hypercholesterolemia, in rabbit, can produce in the cell surface charge and chemistry of arterial endothelium (E) and blood monocytes (M). Weekly, up to 8 weeks, after blood samples were taken for lipid analysis and blood cell preparation, the vasculature was washed free of blood and the endothelial luminal surface (ES) exposed to cytochemical probes for detecting charged groups, sialoconjugates and oligosaccharides. After fixation *in situ*, specimens collected from lesion-prone regions (aortic arch and coronary artery) and vena cava, were processed for electron microscopy. Morphometric analysis of tracer distribution on endothelium of nonlesional and lesional areas occurring in various stages of structural alterations, showed a remarkable resistance of the cell coat to very high level of serum cholesterol. In nonlesional zones the E surface charge and glycoconjugates were not significantly changed. In lesional areas, including those with forming fatty streaks, while cationic sites, galactosyl-, and *N*-acetyl-galactosaminyl residues were not altered whereas mannosyl moieties increased in density. A reduction in anionic groups and sialoconjugates appeared only after advanced extracellular and intracellular accumulation of lipoprotein-derived material and stromal proliferation developed in the intima. Moreover, these ES changes were usually restricted to the relatively rare E cells heavily loaded with lipid inclusions. The modulations were generally paralleled by comparable variations in the M surface. Regardless the extent of surface charge reduction, monocytes continued to migrate and foam cells to egress from the vessel wall. The results suggest that the onset and progression of early intimal lesions are not preceded but followed by significant restricted alterations in cell surface charge and glycoconjugates of arterial endothelium and monocytes.

Key Words *arterial endothelium - monocytes - cell surface charge - glycoconjugates - hypercholesterolemia*

INTRODUCTION

The increasing body of evidence revealing that the inception of atherosclerosis requires neither physical damage to endothelium, nor platelets involvement, has prompted the search for more subtle focal endothelial changes which can be associated with atherogenic tendencies. It seems reasonable to assume that before any so-called early lesions appear, the intimal components, particularly the endothelium, may undergo biochemical and ultrastructural perturbations that generate local tissue reactions leading to lesion development. One of these minute prelesional changes detected was the subendothelial progressive extracellular accumulation of lipoprotein-derived material appearing as phospholipid liposomes rich in unesterified cholesterol (Simionescu *et al.*, 1986) and closely associated with apoprotein B (Mora *et al.*, 1986).

Because the earliest cellular perturbation so far identified has been the focal adherence of mononuclear cells to arterial endothelium (Gerrity, 1981; Hanson *et al.*, 1981; Joris *et al.*, 1983, 1984), and since endothelial cell surface (ECS) seems to be involved in all major physiopathologic events of the vessel wall, we have investigated the *in vivo* changes which hypercholesterolemia may induce in the chemistry of the cell coat (glycocalyx) of both arterial endothelium and blood monocytes. The information so far available on this issue is rather scarce, obtained at various stages of cholesterol diet, and usually reports separately on modifications in ECS staining with Ruthenium red (Gerrity *et al.*, 1977; Lewis *et al.*, 1982), Concanavalin A (Lewis *et al.*, 1982; Weber *et al.*, 1973, 1984) or cationized ferritin (Lewis *et al.*, 1982). As for the monocytes, although they have been shown to respond to a large variety of chemotactic stimuli,

little is known concerning the *in vivo* mechanisms controlling their recruitment and migration into the lesion-prone zones of arterial intima (Gerrity *et al.*, 1985; Schwartz *et al.*, 1985). The chemical changes of the monocyte cell surface during various stages of atherogenesis and their possible relationships with comparable perturbation occurring in parallel in arterial ECS have been virtually unexplored. This is why our present study was addressed concomitantly to the biochemical alterations that experimental hyperlipidemia in rabbit may produce in the ECS of a lesion-prone area such as the aortic arch (Simionescu *et al.*, 1986) and of the blood monocyte occurring either in circulation or interacting with arterial endothelium. The evaluation of such changes was based on their comparison with the chemical mapping established for these two cell types in the normal rabbit (Leabu *et al.*, 1987). Although the experimental atherosclerosis may not be totally relevant to the disease in man, during the diet-induced hypercholesterolemia and subsequent accelerated atherosclerosis, the lipid deposition largely resembles the early intimal changes in atherosclerotic aorta and coronary in humans (Mahley, 1982, 1983).

MATERIALS AND METHODS

Animals and diet

Forty one male adult Chinchilla rabbits 2-3 kg in body weight received for 1-8 weeks a diet of pelleted rabbit chow containing 0.5% cholesterol and 5% butter. Seventeen animals used as controls were fed a standard diet. Animals were sacrificed weekly: blood samples were taken for plasma lipid analysis and for preparing suspensions of blood cells, then the vasculature was washed blood-free for its exposure to the cytochemical probes.

Plasma lipid analysis

Individual rabbit serum was examined for its content in cholesterol and triglycerides using the Sigma reagent Kit (Zlatkis and Zak, 1969). Animals developed rather rapidly a hypercholesterolemia characterized by the presence of β-VLDL as major cholesterol carrier (Mahley *et al.*, 1980; Simionescu *et al.*, 1986). The recorded values determined the selection of animals who respond more uniformly and significantly to the cholesterol-rich diet. The levels of plasma cholesterol were correlated with the changes in the cell surface chemistry of endothelium and blood cells especially the mononuclear elements.

Preparation of blood cells

Suspensions of circulating blood cells were prepared as described for the normal animals (Leabu *et al.*, 1987). In addition, in electron microscopic preparations, we examined the mononuclear cells closely associated with vascular endothelium (adherent or undergoing diapedesis). A special attention was given to foam cells either circulating or immigrating from the vessel wall into the lumen.

Cytochemical probes

From the cytochemical tracers used in normal animals (Leabu *et al.*, 1987), we have selected eight that gave the most consistent and significant results: *hemeundecapeptide* (HUP) pI 4.85 for the visualization of cationic groups, *cationized ferritin* (CF) pI 8.4, for detecting anionic groups, *ferritin hydrazide (FH) to label on the cell surface, oxidized by Na periodate, the sialyl residues not* O-acetylated at C_8 or C_9, *wheat germ agglutinin* (WGA) followed by mucin-gold (M-Au) to localize the *N*-acetyl-neuraminic acid and *N*-acetyl-glucosamine, *Concanavalin A* (Con A) followed by horseradish peroxidase-gold conjugate (HRP-Au), for labeling the mannosyl residues, *Ricinus communis agglutinin* (RCA) followed by lactosaminated bovine serum albumin-gold complex (LacN-BSA-Au) to detect terminal and/or subterminal galactosyl residues, and *galactose-oxidase* followed by *ferritin hydrazide (GO/FH) to label terminal galactosyl and* N-acetyl-galactosaminyl residues. After treatment with *neuraminidase*, the unmasked subterminal galactosyl and *N*-acetyl-galactosaminyl moieties, upon oxidation with GO were marked by FH. The probes were applied as described in the accompanying paper (Leabu *et al.*, 1987).

Tissue processing for ultrastructural cytochemistry

In addition to blood cell suspensions, we examined endothelium of the aorta (arch and thoracic segment), coronary arteries, and vena cava.

Morphometry and statistical analysis

The morphometric analysis was conducted as described in Leabu *et al.* (1987). The sampling was as follows: from the aorta of each of the 58 animals used for these experiments 2-5 blocks were thin-sectioned, and 5-10 sections were examined by electron microscopy. Ten to 50 micrographs were randomly taken from areas found in each of the six lesional stages considered (see Results). Tracer particles were counted on micrographs printed at magnifications of × 80,000 to × 110,000 for each stage of the diet. Depending on the homogeneity and standard deviation of the values obtained for the binding pattern of each tracer at a given lesional stage, tracer particles were counted on actual endothelial length that varied between 30 and 160 μm for CF and FH. For lectins, the endothelial profiles examined were: 559 μm for nonlesional areas and 463 μm for lesional areas from Con A experiments, 71 μm for nonlesional areas and 35 μm for lesional areas from RCA specimens, and 774 μm for nonlesional areas and 632 μm for the lesional zones in WGA experiments. The sample mean ± standard deviation was expressed as a number of tracer particles/μm^2 of membrane surface assuming a section thickness of 70 nm. Statistical significance between data was evaluated by using F-test.

RESULTS

Because of individual variations in the response to the lipid-rich diet, we have selected for our experiments only those rabbits whose plasma level of cholesterol increased significantly and according to the duration of the diet. The investigations on the endothelial cell surface were carried out on animals at 1, 2, 3, 4 and 8 weeks of diet, whereas those on blood cells were focused on weeks 2, 4, and 8.

Plasma lipid and lipoprotein analysis

In animals fed a standard diet the cholesterol level was 35-45 mg/dl serum. The figures increased to 240-300 mg/dl in the first week, 250 to 510 mg/dl in the second week, 800-980 mg/dl in the third week, 1,000-1,200 mg/dl in the fourth week, and 1,400-2,000 mg/dl in the eighth week of

diet. While low density lipoprotein (LDL) content of plasma progressively and markedly decreased, the β-very low density lipoprotein became the major cholesterol carrier. In the latter, the ratio of mass protein content to mass cholesterol content diminished from approximately 1:1.5-2.0 in the first week of diet to about 1:1.1 in the eighth week of the diet.

Chemistry of endothelial cell surface

Endothelia examined - Segments of vessel wall were collected from four regions: *a*) the inner lesser curvature of the aortic arch, as a consistent lesion-prone area, which in our experimental conditions was shown to develop in more than 95% of cases fatty streak lesions (Simionescu *et al.*, 1986), *b*) thoracic aorta, frequently affected by hypercholesterolemia, *c*) coronary arteries (the proximal third of the interventricular branch), and *d*) vena cava thoracica notoriously unaffected by atherosclerosis.

Lesional stages considered - Taking into account the focal nature, the various speed of development, and the resulting polymorphism of the atherosclerotic lesions, with a certain degree of arbitrariness, we classified the ultrastructural appearance of the arterial wall in the lesion-prone areas, into six stages, characterized as follows:
Stage 0 - Non-lesional areas without extracellular liposomes or matrix proliferation. They were represented by any ultrastructurally lesion-free endothelial zone of normal or hypercholesterolemic animals.

Stage I - Non-lesional areas with extracellular liposomes and/or matrix proliferation. In the first two weeks of diet as well as in some nonlesional areas of later stages (weeks 3 to 8), by all ultrastructural criteria the endothelial cells appeared intact. By fluorescent microscopy and electron microscopy we revealed that some apparently intact intima contained a subendothelial accumulation of cholesterol-rich extracellular liposomes (Simionescu *et al.*, 1986, and this paper). Such zones may also contain a sero-fibrinous insudation and/or proliferation of matrix components such as collagen fibers, fragmented elastin, microfibrils and amorphous basal lamina-like material (Simionescu *et al.*, 1986). It was at these locations where mononuclear cells usually began to adhere and migrate into the vessel wall, event that actually marked the transition to the next stage.
Stage II - Sites of mononuclear cell adhesion and migration. The ultrastructure of endothelium was not significantly changed in such areas, though occasionally a tendency to polymorphic appearances was noticed.
Stage III - Areas overlying macrophages and/or foam cells. With the cytological features of a normal appearance, the endothelial cells display however polymorphic shape, some of them covering protruding foam cells became flattened, but without any cell discontinuity, and no obvious open endothelial junctions. Occasionally, some endothelial cells displayed dense bands of actin filaments at their base, enlarged endoplasmic reticulum and Golgi complex.
Stage IV - Endothelial foam cells (EFC). In relatively advanced fatty depositions, in addition to the foam cells derived from monocyte-macrophages and smooth muscle cells,

TABLE I

Cationic ferritin labeling of aortic endothelium in areas with various lesional stages induced by hypercholesterolemia

State of arterial wall		Endothelial features labeled by cationic ferritin						
Structural modifications	Stage	Plasma membrane (particles number/μm²)	Coated pits %	Coated vesicles %	Plasmalemmal vesicles: opened to the lumen %	Plasmalemmal vesicles: lumen associated %	Plasmalemmal vesicles: cytoplasmic %	Multivesicular bodies %
Nonlesional areas								
- Without EL*	0	1623 ± 221	100	33	96	89	23	13
- With EL**	I	1503 ± 432	99	54	77	71	22	21
Lesional areas								
- Sites of mononuclear cell adhesion and diapedesis	II	1418 ± 312	92	ND	92	77	14	ND
Areas overlying foam cells	III	1476 ± 370	83	36	95	90	35	21
Endothelial foam cells	IV	370 ± 288	30	33	41	64	11	15
- Sites of foam cell immigration	V	1074 ± 168	33	18	26	47	19	12

* EL: extracellular liposomes; ** with or without associated matrix proliferation; ND: not determined. The total number of endothelial features counted was: 2017 plasmalemmal vesicles (844 open to the lumen, 573 lumen-associated, and 600 apparently within the cytoplasm), 36 coated pits, 85 coated vesicles, and 67 multivesicular bodies.

some endothelial cells started to participate in the local cleaning of accumulated lipids, becoming loaded with lipid inclusions like any other foam cell (Lupu *et al.*, 1986).

Stage V - Sites of foam cell immigration where the intimal most superficial foam cells (FC) via largely open intercellular junctions egressed into the blood stream. At this level, though still intact and continuous, EC were commonly thin, with a reduced number of plasmalemmal vesicles, but increased amount of microfilaments.

Since by its nature the atherosclerotic process is focal with relatively slow and uneven progression, nonlesional and lesional areas in different stages of evolution could coexist in the same region. Commonly the tissue reaction progressed from the peripheral to the central part of the forming plaque, especially during the fatty streak development. The duration of the fat-rich diet was important for the increasing values of plasma cholesterol, but depending on the regional response of the artery wall; even at late time points we could find areas representing any of the six stages described. This is why we did not make a strict correlation between the number of weeks of diet and the lesional stages considered. However, we could notice that in the first two weeks of diet, stages 0 and I were most frequently encountered. Monocytes attachment to endothelium and diapedesis beginning to take place from the third week on, was a process that continued during the entire period of 8 weeks examined. In these experimental conditions, foam cell formation also started in the third week and continued thereafter, whereas development of endothelial-derived lipid-laden cells and foam cell immigration into the circulation were late events of the fourth to the eighth week of diet corresponding to a cholesterolemia of at least fifty fold higher than the normal. The changes in the chemical moieties of ECS detected with our probes were generally found to be strictly related to the stage of the focal lesion and much less to the level of hypercholesterolemia.

The changes recorded by morphometric analysis were compared on the one hand with the ligand distribution in normolipidemic animals (Leabu *et al.*, 1987), and on the other hand in the hypercholesterolemic rabbits, in the lesion-prone regions the comparison was made between the endothelium of lesion-free areas and that of zones affected by characteristical intimal modifications.

For a comprehensive view of the cell surface changes that characterized a given intimal lesion, the illustrations in this paper were assembled on stages. To emphasize the modifications that a certain residue had undergone during hypercholesterolemia, these were successively described for each chemical component detected. As a result of this, the figure numbers are not necessarily in sequence.

Cell surface charge - Anionic sites. As compared with the normolipidemic animal, in the hyperlipidemic rabbit the CF binding was at values only slightly lower (less than 15% in most cases), and the decoration of plasma membrane remained very dense along the entire period (8 weeks) of the diet (Table 1). The only exception were the endothelial lipid-laden cells, as further described. The density of CF

Figures 1 to 6 Hypercholesterolemic rabbits: endothelium of aortic arch in nonlesional areas (stage I).

FIGURE 1 In regions containing subendothelial extracellular liposomes (el) endothelial cell surface displays a relatively uniform distribution of dense CF-binding sites on plasma membrane (p) and most plasmalemmal vesicles (v). m: microfibrils; bl: basal lamina-like material. × 52,000.

FIGURE 2 FH-detectable sodium periodate-oxidized sialyl residues appear homogeneously distributed on plasma membrane (p), but only occasionally tracer particles are found in plasmalemmal vesicles (v). × 108,000.

FIGURE 3 Cationic groups as marked by HUP reaction product occupy as a continuous monolayer plasma membrane (p), what appears to be a coated pit (cp) and all plasmalemmal vesicles (v) open to the lumen (l). On the latter, it is obvious the adsorptive type of binding. n: nucleus. × 59,000.

FIGURE 4 WGA-binding sites (*N*-acetyl neuraminic acid and *N*-acetyl glucosamine) are generally at low density on most endothelial cells (e). However, some endothelial cells (e) are on the contrary extremely rich in such moieties on their plasmalemma (p) without showing any other distinct structural feature. j: junction between the two adjoining cell types. × 64,000.

FIGURE 5 Mannosyl residues detected with Con A/HRP-Au are well represented on plasma membrane (p) and some coated pits (cp) but to a lesser extent on plasmalemmal vesicles (v). × 112,000.

FIGURE 6 Terminal and/or subterminal galactosyl moieties indirectly visualized with RCA/LacN-BSA-Au are very dense on plasma membrane (p) and very rare in vesicles (v). A characteristic high density occurs on cytoplasmic folds (f). × 54,000.

Abbreviations used in figures - bl: basal lamina (basal lamina-like material); *e*: endothelial cells; *el*: extracellular liposomes; *cp*: coated pit; *l*: lumen; *p*: plasma membrane; *v*: plasmalemmal vesicle.

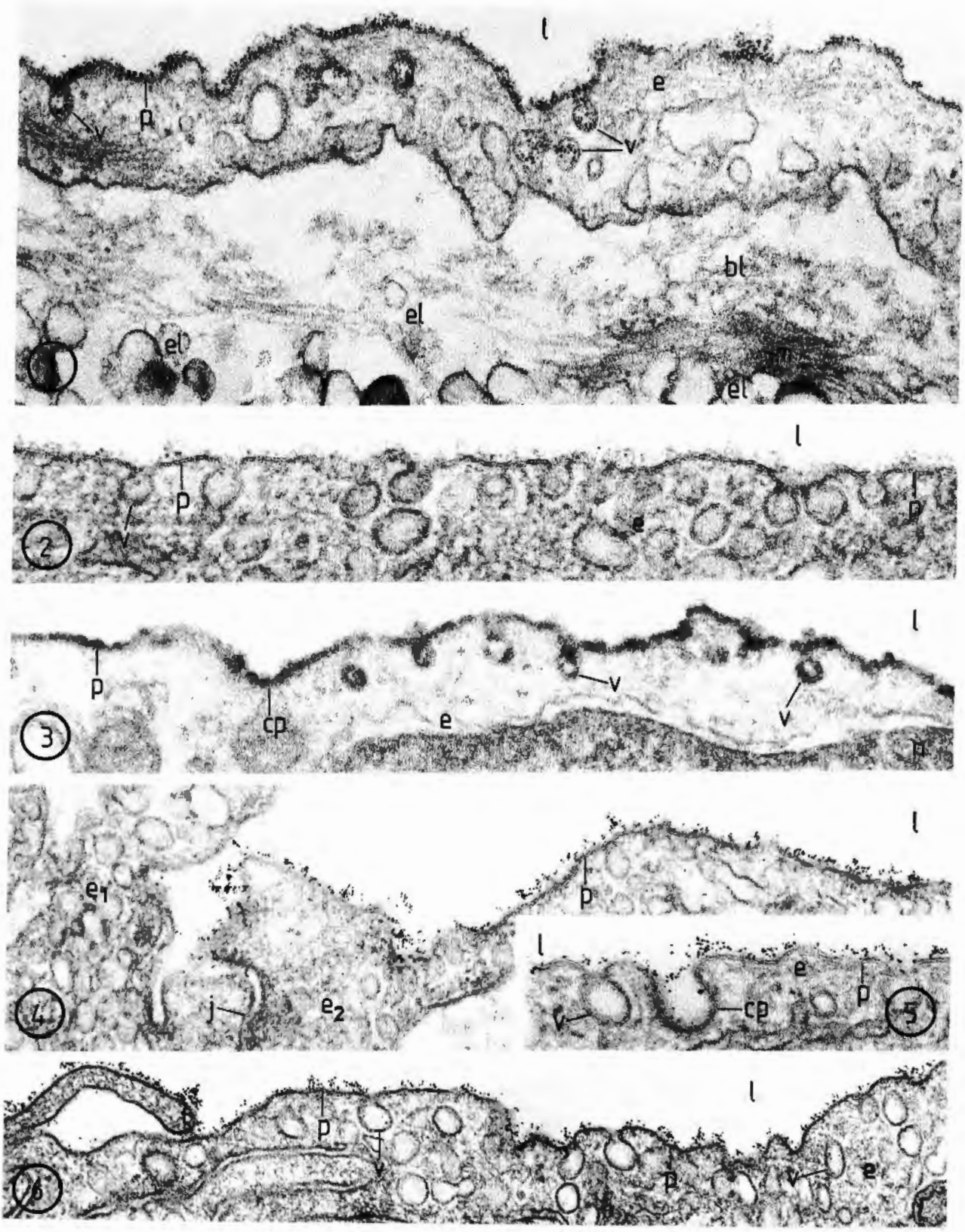
l
p
v
e
v
bl
el
el
el
l
p
v
2
p
e
l
p
cp
v
v
3
e
l
e1
p
4
j
e2
l
e
p
v
cp
5
l
p
v
6
p
l
p
v
e

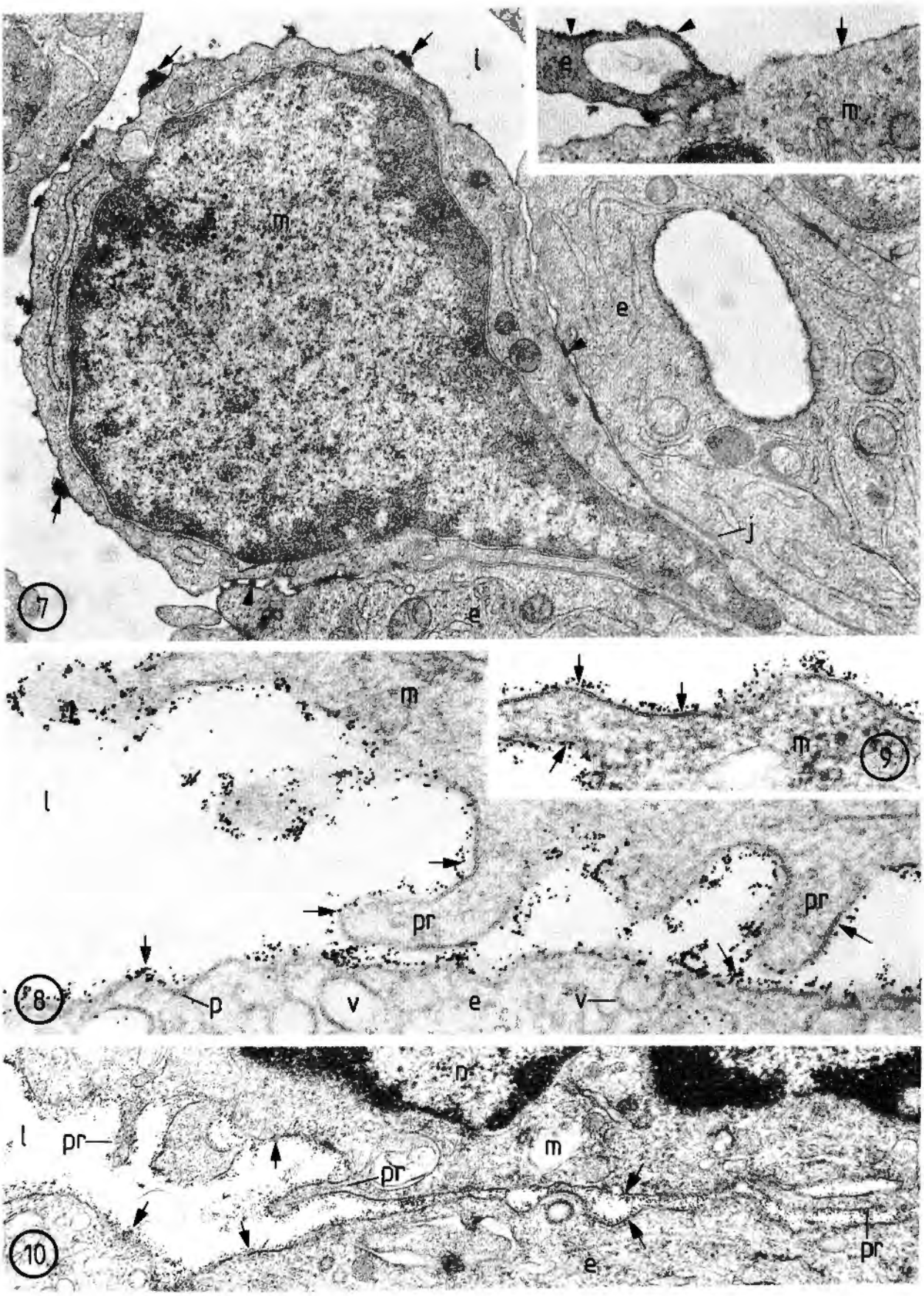
l
m
e
j
7
m
l
pr
p
v
e
v
8
m
9
n
l
pr
m
pr
10
e
pr

TABLE 2

Ferritin hydrazide labeling of sodium periodate-sensitive sialyl residues of aortic endothelium in areas with various lesional stages induced by hypercholesterolemia

Endothelial features	State of arterial wall					
	Nonlesional area without EL* (Stage 0)	Nonlesional area with EL* (Stage I)	Sites of mononuclear cell adhesion (Stage II)	Areas overlying foam cells (Stage III)	On endothelial foam cells (Stage IV)	Sites of foam cell immigration (Stage V)
Plasma membrane**	948 ± 130	1151 ± 219	ND	785 ± 155	684 ± 115	722 ± 194
Plasmalemmal vesicles‡	23.0 (217)	23.1 (785)	ND	20.8 (420)	17.1 (152)	20.3 (74)

*EL: extracellular liposomes; **expressed as FH particles/μm^2 membrane area ± standard deviation of the mean; ‡labeled vesicles usually contained 1-2 FH particles; in parentheses, the number of vesicles counted (the relatively low figure for stage V, is due to the rarity of these events; so is explained the lack of significant counts for stage II); §with or without concurrent matrix proliferation; ND: not determined, due to the variety of these events (estimated qualitatively only).

labeling of plasma membrane, showed statistically nonsignificant differences between nonlesional and lesional zone (Figs. 1 and 12), with the exception of the cell coat of the endothelial foam cells containing a high number of lipid droplets. On these cells the CF density was diminished by ~80% as compared with normal or with areas in stage 0 from hypercholesterolemic animals (Table 1) and CF particles appeared mostly in small clumps attached to plasma membrane (Fig. 17). At sites of foam cell immigration into the lumen the CF density varied from normal (Fig. 21) to a reduction of ~30%; in general, the anionic sites density on ECS was higher than on the adjacent monocytes. During monocyte diapedesis, at contact sites between EC and monocytes, there were fewer anionic sites especially on the monocyte cell surface where they usually formed small clusters (Fig. 7). The endothelial-monocyte contact in many cases was not occludent since CF particles could penetrate the space and reach the subendothelial spaces. In nonlesional areas containing EL (stage I) as well as in zones of foam cell formation (stage III) while most coated pits appeared marked by CF, an increase of almost 80 to 100% of decoration of multivesicular bodies was noticed (Table 1). Labeling of plasmalemmal vesicles was significantly diminished in EFC and at sites of FC immigration. Similar CF decoration pattern was observed both in aortic and in coronary endothelium.

The density and distribution of CF binding sites on ECS did not change markedly with the increasing plasma cholesterol concentration. Comparing with the binding density of 1,700 CF/μm^2 in the first week of diet when cholestero-

Figures 7 to 10 Exemplify the distribution of some probes on the cell surface of aortic endothelium in a lesion-prone area of the aortic arch, characteristic for the stage II

FIGURE 7 Monocyte (m) found between two endothelial cells (e) apparently entering the intima; image taken from a specimen at the 8th week of diet, showing patchy CF labeling of both monocyte (arrows) and endothelium (arrowheads). Inset: detail of a monocyte (m) migrating into intima, at the second week of diet; while CF binding sites are scarce on MCS (arrow), they have a normal distribution on the adjacent endothelial cell (arrowheads). j: junction. × 19,000; inset: × 28,000.

FIGURE 8 At the interface between a monocyte (m) and an endothelial cell (e) the distribution of Con A-detectable mannosyl moieties (arrows) is virtually similar to that of controls. pr: cytoplasmic projections. × 120,000.

FIGURE 9 On circulating monocytes (m), the Con A-binding sites (arrows) are generally comparable with the pattern observed on adherent monocytes. × 127,000.

FIGURE 10 The adhering monocyte (m) as well as the opposed endothelial cell display on their surface an RCA binding pattern (arrows) similar to that occurring on these cells in the normolipidemic rabbit. pr: cytoplasmic protrusions; n: nucleus. × 22,000.

TABLE 3

Ferritin hydrazide labeling of sodium periodate-sensitive sialyl residues of aortic endothelium in areas with various lesional stages, as a function of weeks of diet and plasma cholesterol level

State of arterial wall		Weeks of diet				
		Average plasma cholesterol concentration (mg/dl)				
Structural modifications	Stage	1 240-300	2 250-510	3 800-980	4 1,000-1,200	8 1,400-2,000
Nonlesional areas						
Without EL.**	0	962 ± 108	1039 ± 109	820 ± 124	ND	ND
With EL	I	1290 ± 240	1114 ± 149	1153 ± 79	1134 ± 141	995 ± 296
Lesional areas						
Sites of mononuclear cell adhesion and diapedesis	II	ND	ND	ND	ND	ND
Areas overlying foam cells	III	ND	847 ± 76	866 ± 155	770 ± 157	743 ± 121
Endothelial foam cells	IV	ND	ND	703 ± 131	596 ± 83	699 ± 112
Sites of foam cell immigration	V	ND	ND	539 ± 73	1002 ± 111	743 ± 150

Expressed as FH particles/μm^2 membrane area ± standard deviation of the mean; **EL: extracellular liposomes; *with or without concurrent matrix proliferation; ND: not determined due to the rare events seen (estimated qualitatively, only).

lemia was 250 mg/dl, in the fourth and eighth weeks, when plasma cholesterol reached 1,000 and 1,500-2,000 mg/dl, respectively, the CF binding density varied within an insignificant range (usually less than 10%).

Cationic sites. The reaction product of HUP used for detecting the cell surface cationic sites, labeled the aortic endothelium of both nonlesional and lesional areas as an adsorbed continuous layer (~30 nm thick) the plasma membrane, coated pits and all plasmalemmal vesicles open to the lumen (Figs. 3, 11 and 16). This decoration pattern was not conspicuously changed by the level of hypercholesterolemia, regardless the type of local lesion. The findings revealed that during hypercholesterolemia the net cell surface charge of endothelial cells remained apparently unmodified, both in nonlesional and lesional regions. While the distribution of the cationic groups was still unchanged, a drastic reduction in CF-detectable anionic groups was a hallmark of endothelial foam cells loaded with lipid droplets. As compared with the control experiments, in stages I and III the CF endocytosis by endothelium was enhanced about 7 folds (21% labeled multivesicular bodies versus 3% in controls).

Cell surface sialoconjugates - As detected with ferritin hydrazide (FH), the sodium periodate-sensitive sialyl resi-

Figures 11 to 15 Cell surface of aortic endothelium overlying monocyte derived macrophages or foam cells in regions of forming fatty streaks (stage III)

FIGURE 11 Cationic groups as visualized by HUP-reaction product appear as a continuous layer on plasma membrane (arrows) and mark also plasmalemmal vesicles (v). bl: basal lamina-like material; mc: macrophage; en: elastin. × 25,000.

FIGURE 12 Anionic groups marked by CF are almost homogeneously distributed on plasma membrane (p), also labeling coated vesicles (cv) and most of plasmalemmal vesicles (v). j: junction, not penetrated by the probe; mc: macrophage. Inset: a large proportion of multivesicular bodies (mv) are labeled by endocytosed CF particles (arrowheads). × 72,000; inset: × 84,000.

FIGURE 13 FH-labeled sodium periodate-oxidized sialic acids are only slightly decreased in density on plasma membrane (p) while plasmalemmal vesicles (v) are not marked. × 81,000.

FIGURE 14 Mannosyl residues detected by Con A are well represented on plasma membrane (arrows). fc: foam cell; li: lipidic inclusions. × 54,000.

FIGURE 15 In some locations, endothelial cells (ec) overlying foam cells (fc) display disorganized intercellular junctions (j) with tracer particles (arrowheads) (in this case RCA/LacN-BSA-Au) penetrating into the subendothelial space (ss). On endothelial cell surface (p) RCA-binding sites show a distribution comparable with that of normal animals. pr: cytoplasmic protrusions of the foam cell (fc). × 32,000.

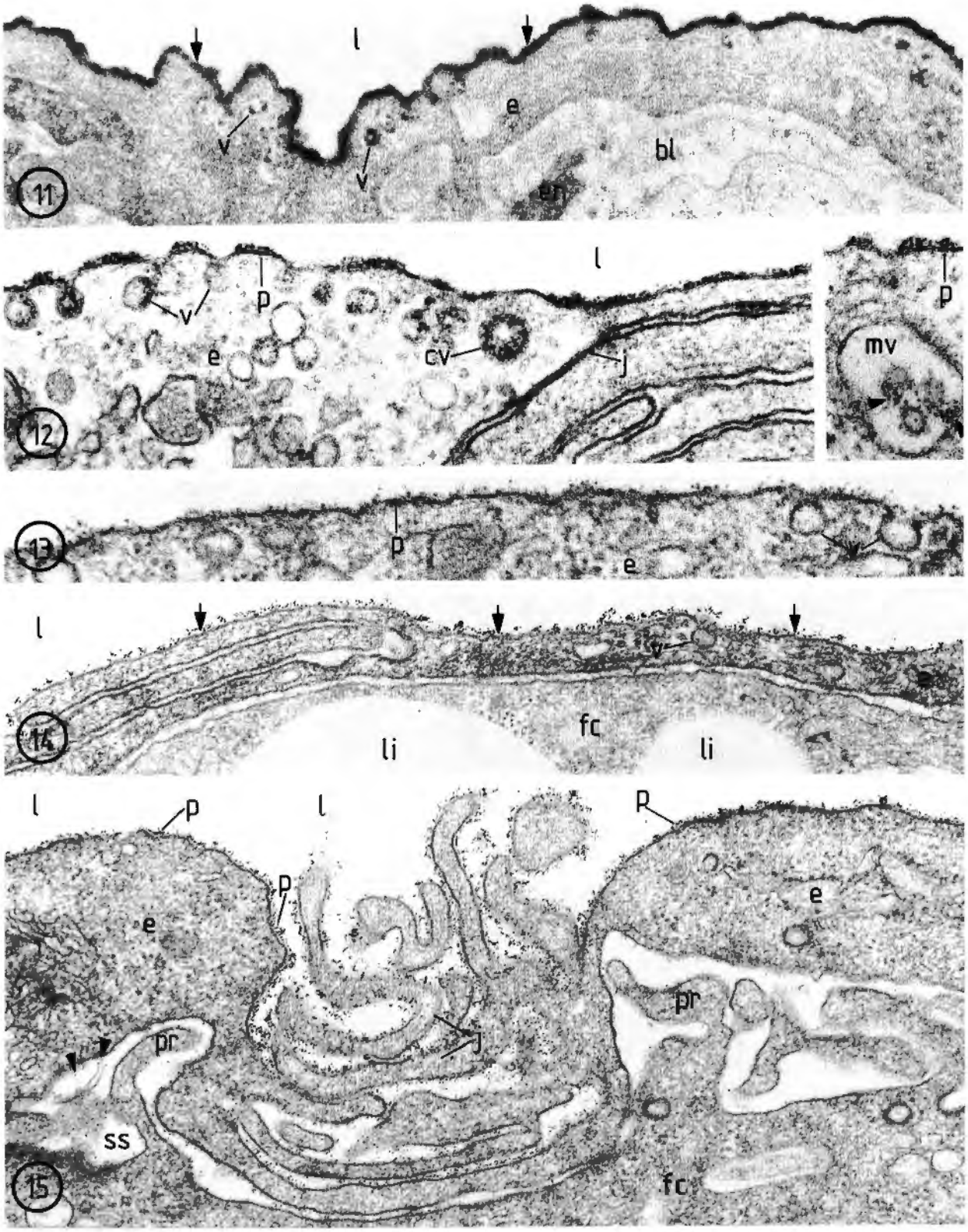
11
l
v
v
e
bl
er
12
l
v
p
e
cv
j
p
mv
13
p
e
14
l
v
fc
li
li
15
l
p
l
p
p
e
e
pr
pr
j
ss
fc

TABLE 4

Lectin binding on aortic endothelium in areas with various lesional stages induced by hypercholesterolemia

State of arterial wall		WGA			Con A			RCA		
Structural modifications	Stage	Plasma membrane (particles /μm²)	Coated pits %	Plasma-lemmal vesicles %	Plasma membrane (particles /μm²)	Coated pits %	Plasma-lemmal vesicles %	Plasma membrane (particles /μm²)	Coated pits %	Plasma-lemmal vesicles %
Nonlesional areas										
Without EL*	0	84 ± 50	59	12	2336 ± 638	80	38	1035 ± 82	ND	10
With EL	I	81 ± 52	50	8	2837 ± 1244	90	42	1103 ± 226	ND	9
Lesional areas										
- Sites of mononuclear cell adhesion and diapedesis	II	ND			2586 ± 883	ND	31.2	ND		
Areas overlying foam cells	III	77 ± 43	33	7	2706 ± 628	75	33	1004 ± 44	ND	ND
- Endothelial foam cells	IV	68 ± 33	ND	5	3333 ± 929	81	39	1711 ± 261	ND	11
- Sites of foam cell immigration	V	ND			ND			1550 ± 376	ND	10

* EL: extracellular liposomes; ND: not determined.

dues of plasma membrane in nonlesional areas of hypercholesterolemic animals appeared to be either unchanged or slightly increased (948 and 1151 for stages 0 and I, respectively) as compared with the normally fed rabbits (885 FH particles/μm²) (Fig. 2). In lesional areas with stages III (Fig. 13) and V, the FH labeling density was only slightly diminished (12-17%) (Table 2). A relatively more pronounced reduction was recorded on endothelial foam cells (~25%) (Fig. 17, inset). The extent of FH labeling of plasmalemmal vesicles generally paralleled the slight decrease of FH decoration of plasma membrane (Table 2). The figures in Table 3 show a very significant finding namely that the degree of FH labeling of the ECS of a given lesional (or nonlesional) area is practically the same regardless the duration of the diet and the values of plasma cholesterol concentration. Only minor modifications in the density of neuraminidase-sensitive residues were recorded: the average number of FH particles/μm² was 239 ± 70 in stage 0, 268 ± 56 in stage I, 201 ± 71 in stage III and 203 ± 54 in stage V. An ~30% reduction was noticed only on EC-derived foam cells (stage IV).

These observations revealed that on the ECS the FH-detectable sialoconjugates were not or very little affected, irrespective of the length of diet or degree of hypercholesterolemia.

Cell surface oligosaccharides - None of the three groups of residues labeled by the lectins used seemed to be markedly altered by hypercholesterolemia. However, each class of these moieties seemed to react differently to the elevated serum lipids (Tables 4 to 7). One striking finding was the response to hypercholesterolemia of WGA-detectable residues. Along the entire length of the diet, both in regions uninvolved and in regions developing a marked extra-, and intracellular accumulation of lipids two kinds of areas could be seen: areas in which aortic ECS had a WGA binding pattern comparable to that in control specimens (Figs. 4 and 18 and Table 6), and areas of much enriched (by ~8 times) density of WGA-detectable moieties (Fig. 4 and Table 7). The general ultrastructure of the EC was quite similar in both areas. A more detailed analysis of the latter zones is under current investigation. Preliminary estimates suggest that the frequency of zone with enriched WGA-binding sites was augmented with the progression of the hypercholesterolemia. Mannosyl residues marked by Con A/HRP-Au generally showed a significant increase (by 20-40%) in density on EC plasma membrane, that appeared to be proportional to the advancement of focal lesions (e.g. on EFC the increase could reach 50-60% as compared with normolipidemic animals, and to 30-40% vs nonlesional areas of EC in hypercholesterolemic rabbits) (Table 4, Figs. 5, 8, 9, 14, 19 and 23). The values of Con A binding to EC plasma membrane remained high along the entire duration of our experiments (Table 5). The degree of labeling of coated pits and plasmalemmal vesicles remained generally unchanged (Table 4). As compared with control animals, the terminal and/or subterminal galactosyl residues detec-

ted by RCA/LacN-BSA-Au displayed an almost unchanged density on plasma membrane, as well as the extent of labeling of plasmalemmal vesicles (Table 4 and Figs. 6, 10 and 15). Relative to the normal animal, the terminal galactosyl and *N*-acetyl-galactosaminyl residues that galactose oxidase rendered labelable with FH, appeared unaffected on plasma membrane of nonlesional areas (46-48 FH particles/μm^2), and only slightly reduced on endothelial foam cells (stage IV) (~33 FH particles/μm^2). An unexpected finding was the increase (by 50-65%) of RCA binding sites on endothelial foam cells as well as on ECS at sites of foam cell immigration (Table 4, and Figs. 6, 20 and 22). This suggested that, in our experimental conditions, hypercholesterolemia had no cytochemically detectable detrimental effects on the glycoproteins bearing the moieties labeled by Con A, WGA and RCA. The density on ECS was increased almost uniformly for Con A, regionally for WGA and virtually unchanged for RCA binding sites. The binding pattern of the probes used, observed on the aortic endothelium, was generally similar to that detected on the endothelium of coronary arteries.

In hyperlipidemic animals the endothelium of vena cava did not show remarkable alterations in the distribution of the binding sites for the tracers used. Their topography and density were largely comparable to the normolipidemic rabbits. For example, the FH-labelable sialyl residues/μm^2 of membrane surface were 1282 ± 106 in the second week and 1359 ± 144 in the eighth week of diet as compared with 1427 ± 140 in controls. The neuraminidase-sensitive residues showed binding sites values of 314 ± 30 in normal, 392 ± 58 in the second week and 393 ± 73 in the eighth week of diet.

Chemistry of monocyte cell surface

Though other leukocytes were also occasionally seen adhering to (but not migrating through) endothelium, we focused our observations on the mononuclear cells, the most numerous blood elements which in these hypercholesterolemic animals were interacting with the arterial endothelium. Mononuclear leukocytes were examined both in the circulating blood and when associated with the arterial endothelium. The latter were either beginning to adhere to, in close opposition to endothelium or migrating through open endothelial junctions into the aortic intima. These juxta-endothelial cells exhibited the ultrastructural features traditionally ascribed to blood-born monocytes: a relatively large, reniform or indented nucleus, relatively small dense granules often located near the nuclear indentation, prominent endoplasmic reticulum and Golgi complex, and frequent cytoplasmic processes. Such cells were much more often encountered on nonlesional area containing subendothelial EL and on EC of lesional zones, and their frequency

TABLE 5

Concanavalin A binding on aortic endothelium in areas with various lesional stages, as a function of weeks of diet and plasma cholesterol level

State of arterial wall		Weeks of diet				
		Average plasma cholesterol concentration (mg/dl)				
Structural modifications	Stage	1 240-300	2 250-510	3 800-980	4 1,000-1,200	8 1,400-2,000
Nonlesional areas						
· Without EL*	0	2080 ± 631	2594 ± 463	2348 ± 685	ND	ND
· With EL	I	ND	ND	1857 ± 380	4283 ± 941	2419 ± 387
Lesional areas						
· Sites of mononuclear cells adhesion and diapedesis	II	ND	ND	1836 ± 443	3087 ± 736	ND
· Areas overlying foam cells	III	2056 ± 324	2664 ± 501	2709 ± 509	3679 ± 860	2470 ± 463
· Endothelial foam cells	IV	ND	ND	2800 ± 714	3730 ± 893	2761 ± 594
· Sites of foam cell immigration	V			ND		

EL: extracellular liposomes; ND: not determined.

TABLE 6

WGA binding on aortic endothelium in areas with various lesional stages, as a function of weeks of diet and plasma cholesterol level

State of arterial wall		Weeks of diet				
		Average plasma cholesterol concentration (mg/dl)				
Structural modifications	Stage	1 240-300	2 250-510	3 800-980	4 1,000-1,200	8 1,400-2,000
Nonlesional areas						
· Without EL*	0	84 ± 53	103 ± 46	59 ± 35	106 ± 53	ND
· With EL	I	ND	ND	57 ± 51	59 ± 17	133 ± 44
Lesional areas						
· Sites of mononuclear cells adhesion and diapedesis	II			ND		
· Areas overlying foam cells	III	ND	ND	81 ± 44	63 ± 36	124 ± 31
· Endothelial foam cells	IV	ND	ND	67 ± 27	54 ± 34	89 ± 39
· Sites of foam cell immigration	V			ND		

*EL: extracellular liposomes; ND: not determined.

appeared to increase with the duration of the diet. Other leukocytes (lymphocytes, neutrophils) were also seen in positions comparable to those described for monocytes, but they were in minority. At these stages platelets were usually not seen on ECS.

In the absence of specific biochemical markers, the data reported hereafter were collected only on those leukocytes which, by ultrastructural criteria, were unequivocally identified as monocytes. This had the advantage of more reliable data, but reduced markedly the sampling for stage II, as seen in most tables. Hypercholesterolemia affected in various degrees the surface chemistry of different blood cells (Colceag *et al.*, manuscript in preparation); among these, monocytes appeared to he more sensitive than the others. The monocyte margination and migration was a continuous process that took place irrespective of the intensity of

Figures 16 to 20 Tracer binding on the luminal surface of endothelial cells loaded with lipid inclusions (aortic arch, areas in stage IV)

FIGURE 16 Cationic groups visualized through HUP appear as a continuous layer of reaction product delineating plasma membrane (p) and open plasmalemmal vesicles (v). li: lipid inclusions. × 50,000.

FIGURE 17 CF-detectable anionic sites appear markedly reduced in number and clustered (arrowheads). Some plasmalemmal vesicles (v) are still marked by the tracer. li: lipid inclusions. Inset: FH-labeled sodium periodate-oxidized sialyl residues are diminished in number on plasma membrane (p), while most plasmalemmal vesicles (v) are still unmarked. × 49,000; inset: × 127,000.

FIGURE 18 WGA-binding sites (arrowheads) are rare as in controls. li: lipid inclusion. × 54,000.

FIGURE 19 Con A-detected mannosyl moieties are generally very well represented on plasma membrane (p), including cytoplasmic folds (f), while vesicles (v) remain mostly unlabeled. li: lipid inclusion. Inset: detail of Con A decoration of plasma membrane (p), coated pits (cp) and coated vesicles (cv); a plasmalemmal vesicle lacking tracer labeling (v). × 43,000; inset: × 127,000.

FIGURE 20 Galactosyl residues as revealed by RCA/LacN-BSA-Au labeling occur on plasma membrane (p) usually at a density higher than in normolipidemic animals. Plasmalemmal vesicles (v) are mostly unmarked. Note the marked enlargement of rough endoplasmic reticulum (er) containing an amorphous material. li: lipid inclusion. × 42,000.

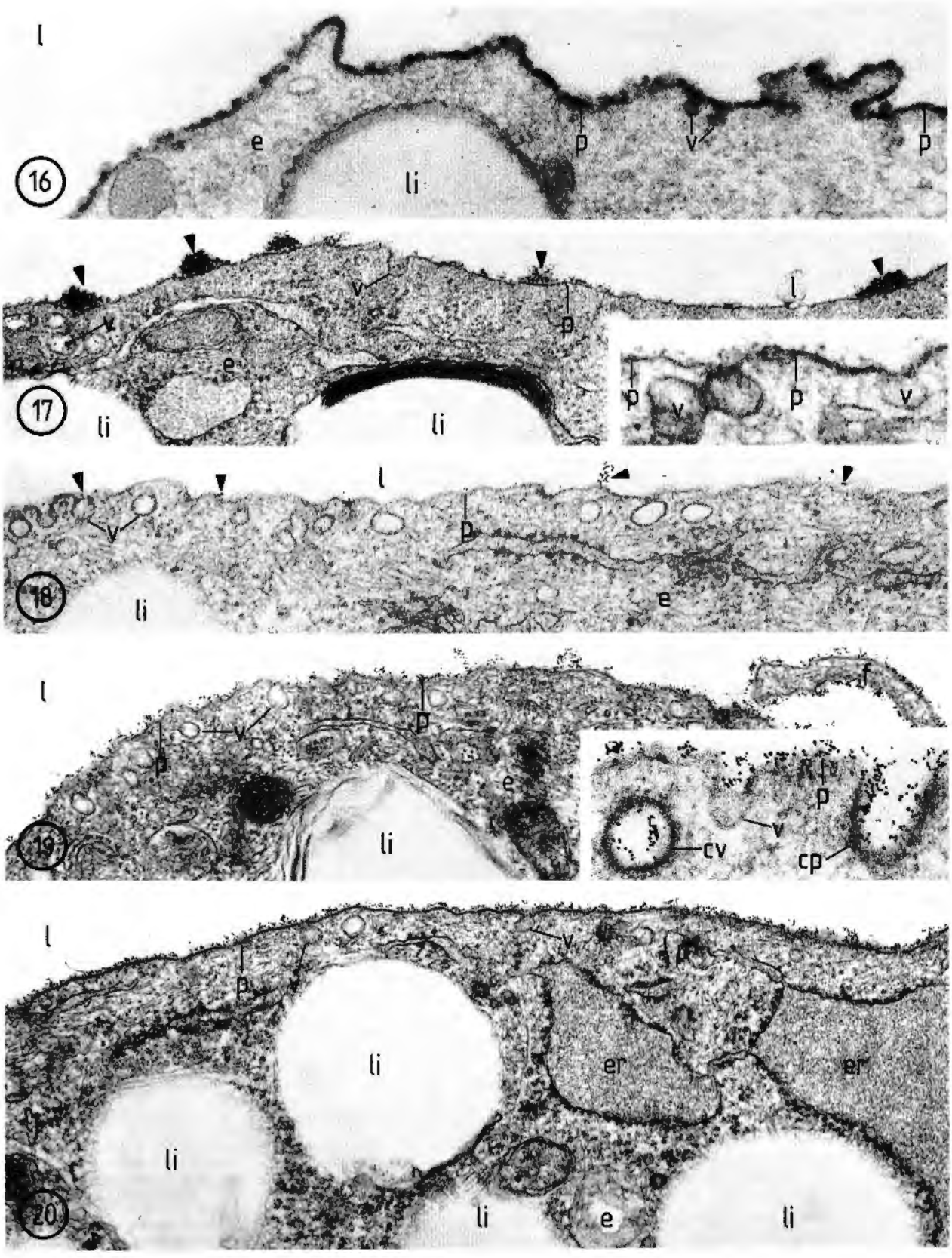
l
e
p
v
p
16
li
v
v
p
l
e
17
li
li
p
v
p
v
l
p
v
18
li
e
l
v
p
f
19
p
v
p
e
li
cv
v
p
cp
l
v
p
li
er
er
li
li
20
li
e
li

changes in the charge or glycoconjugates of ECS and monocyte cell surface (MCS). In general, these modifications reflected more closely the degree of hypercholesterolemia and paralleled those of the ECS. In the first weeks of diet, and the first wave of monocyte attaching to the endothelium (usually the third week), the distribution of CF-detectable anionic sites and FH-labeled sialyl residues was very little or not significantly modified. With the increasing levels of plasma cholesterol, the acidic group of MCS appeared in reduced number and as randomly distributed patches. Large amounts of CF were endocytosed. Concomitantly the reduction in FH-detectable sialic acids was only little altered. At the eighth week, the FH decoration pattern was frequently almost similar to that of normolipidemic animals. However a reduction was noticed in the FH-detectable residues after the galactose oxidase treatment (from 626 ± 115 particles/μm^2 in normolipidemic animals to 217 ± 61 at the eighth week of diet). To a certain extent, comparable modifications were visible on the other blood cells, especially at the eighth week of diet. There were not cytochemically detectable differences in the changes of cell surface chemistry induced by hypercholesterolemia in the circulating monocytes versus those occurring close to or attached to endothelium (Figs. 8, 9, 10 and 22).

Among the lectin binding sites on monocytes, we recorded a diminished labeling by WGA/M-Au, a less significant change in the decoration with Con A/HRP-Au, and an unexpected 50 to 100% increase in RCA-detectable glycoconjugates in the late time of diet (Table 8). As illustrated in Table 9, hypercholesterolemia altered in variable extent the binding sites for the three lectins used on the other blood cell types (Colceag *et al.*, manuscript in preparation).

TABLE 7

Wheat germ agglutinin binding in regions of aortic endothelium with enriched WGA-detectable residues, in hypercholesterolemic rabbits

State of arterial wall		Plasma membrane	Coated pits	Plasma-lemmal vesicles
Structural modifications	Stage	(particles /μm^2)	%	%
Nonlesional areas				
- Without EL*	0	447 ± 248	50	5.5
- With EL	I	593 ± 294	ND	14.3
Lesional areas				
- Sites of mononuclear cells adhesion and diapedesis	II	ND		
- Areas overlying foam cells	III	351 ± 74	ND	16.7
- Endothelial foam cells	IV	499 ± 190	ND	8
- Sites of foam cell immigration	V	ND		

*EL: extracellular liposomes; ND: not determined.

TABLE 8

Lectin binding on monocytes of the hypercholesterolemic rabbit (number of tracer particles/μm^2 of membrane surface ± SD of the mean)

	Stages of the diet		
Lectin/Tracer	Normal	Second week	Eighth week
WGA/M-Au	1108 ± 61	359 ± 34	287 ± 94
Con A/HRP-Au	1082 ± 139	764 ± 165	942 ± 198
RCA/LacN-BSA-Au	1488 ± 97	1044 ± 77	2869 ± 57

FIGURE 21 CF-binding pattern on the cell surface of aortic endothelium (e) at a site of what is interpreted as egress from the vessel intima of a foam cell (fc) (eighth week of diet). Note the normal distribution of the CF-detectable anionic sites on ECS (arrows) in contrast to the rare or absent binding sites on FCS (arrowheads). The space between the two cells is permeated by tracer particles (t). The surface of the foam cell contains numerous cytoplasmic protrusions like the one in (pr). li: lipid inclusion; vc: endocytic vacuole containing CF. × 54,000.

FIGURE 22 The distribution of RCA-detectable galactosyl residues appears to be quasinormal on ECS (arrows), MCS (arrowheads) and on the plasma membrane (p) of an adherent foam cell (fc). The latter extends pseudopodes (pp) interposed between endothelium and monocyte. g: granule; li: lipid inclusion. × 22,000.

FIGURE 23 Con A-labeled mannosyl moieties are well represented (normally at density higher than in controls) on the circulating foam cell (fc), plasma membrane (p) and cytoplasmic protrusions (pr). × 131,000.

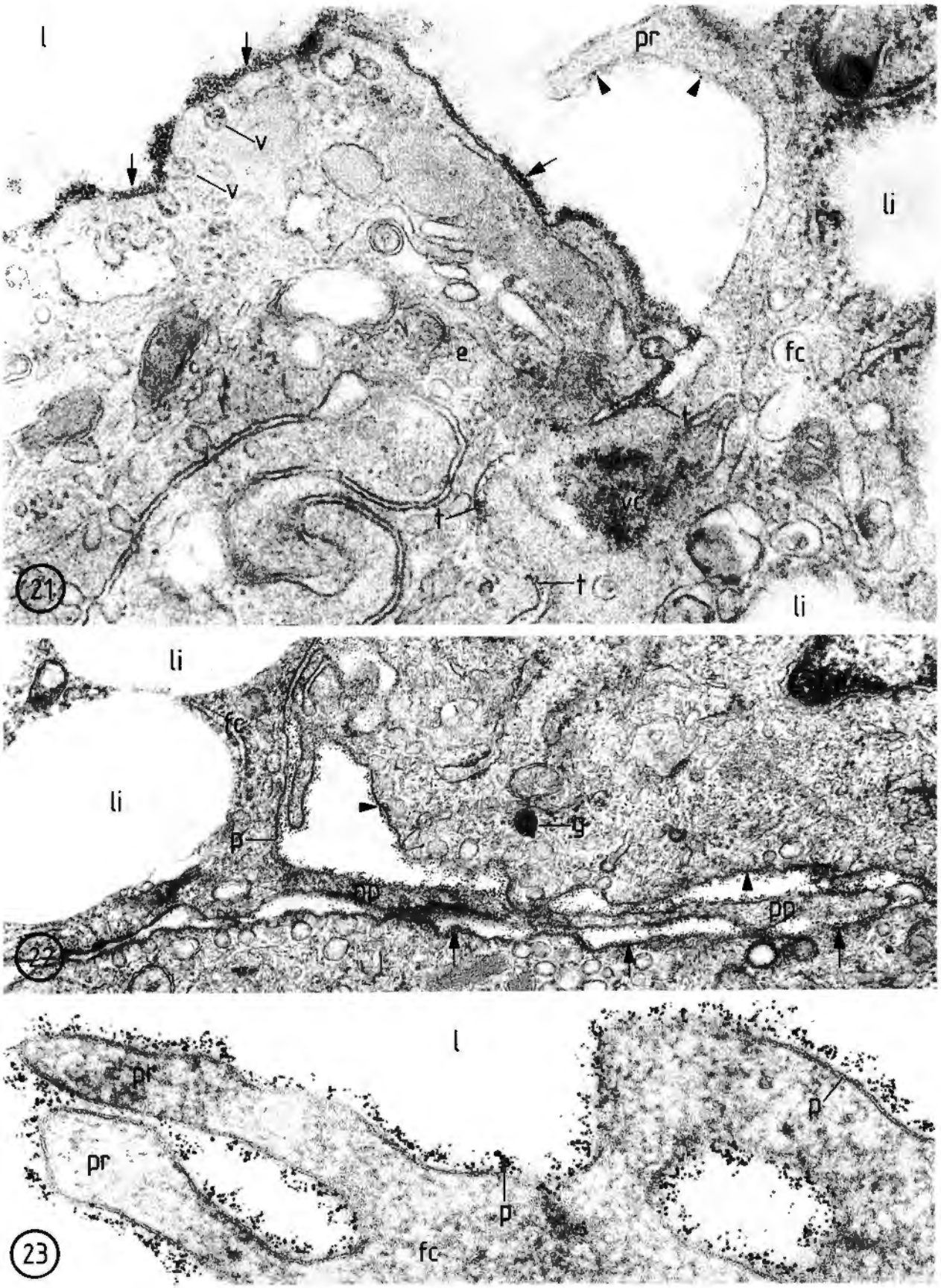
l
pr
v
v
li
e
fc
c
t
vc
t
t
21
li
li
fc
li
g
p
pp
pp
22
l
pr
p
pr
p
fc
23

TABLE 9

Lectin binding on blood cells of hypercholesterolemic rabbit (eighth week of diet)
(number of tracer particles/μm^2 of membrane surface ±SD of the mean)

Cell type	WGA/ M-Au	RCA/ LacN-Alb-Au	Con A/ HRP-Au
Monocyte	287 ± 94	2868 ± 103	942 ± 198
Lymphocyte	260 ± 94	2540 ± 26	814 ± 12
Neutrophil	580 ± 111	3283 ± 11	1379 ± 148
Eosinophil	521 ± 78	2050 ± 36	ND
Erythrocyte	787 ± 69	3219 ± 180	616 ± 98

Cell surface chemistry of immigrating foam cells

In stage V, some subendothelial foam cells heavily loaded with lipid inclusions egressed from the vessel wall into the lumen by progressively opening the intercellular junction of the overlying endothelium (Fig. 21). When detected in these tracer experiments, the cell surface of the immigrating foam cells protruding into the vessel lumen was labeled. In addition, foam cells completely freed in the arterial lumen but still associated with the endothelial surface were also available to the probes used. In most cases, FC occupying an open endothelial junction were labeled by the tracer at intensities comparable or lower than that on the neighbouring endothelial cells (Fig. 21). No platelets were seen interacting with the exposed or immigrating foam cells. Under a certain variation, once a FC was almost freed into the lumen it lost most of its CF binding sites (Fig. 21) as well as FH-detectable sialyl residues (509 ± 130 in the third week, 745 ± 136 in the fourth week and 489 ± 190 in the eighth week of diet). However, the residues labeled by Con A and RCA were usually unchanged (Figs. 22 and 23). Modulation in WGA binding was less obvious. At the level of a patent junction accommodating a FC, in contrast to the luminal ECS, the junctional endothelial surface had very scarce or no CF binding sites (Fig. 21).

DISCUSSION

General

Although high concentrations of cholesterol (at levels not found in man) are used to induce hypercholesterolemia and accelerated atherosclerosis in rabbit, this animal model is thought to produce data relevant to the disease as it occurs in humans, especially on early changes dominated by lipid accumulation in the arterial intima (Wissler and Vesselinovitch, 1968; Mahley, 1982, 1983; Simionescu *et al.*, 1986). Such an approach is based on the assumption that lower levels of hypercholesterolemia over longer time periods will lead to similar results. Beta-migrating very low density lipoprotein, that is much increased in these rabbits, was proved to be a potent atherogenic lipoprotein (Goldstein *et al.*, 1980; Mahley *et al.*, 1980; Simionescu *et al.*, 1986). The arterial modifications observed in our eight-week hypercholesterolemic rabbit appeared as a condensed atherogenesis leading to fatty streak formation and its later conversion to intermediary lesions and fibrous plaque, as described in other species as well (Wissler and Vesselinovitch, 1968; Mahley, 1982, 1983; Faggiotto *et al.*, 1984; Faggiotto and Ross, 1984; Ross, 1986).

The validity of our experimental system in which the aortic arch, particularly its lesser inner curvature was sampled, has been emphasized by observations on more than 300 rabbits we have used for various investigations of the atherogenic process.

Under the inherent limitations of the cytochemical procedures in general, for what was aimed at in this study, such techniques are yet the only capable to reveal difference in the distribution of some moieties at a level of the tiny adjacent microdomains of the endothelial cell surface (Simionescu *et al.*, 1982; Simionescu and Simionescu, 1986). We have purposely chosen mostly two step methods employing a particulate second tracer in order to allow quantification through morphometry and statistical analysis.

ECS and MCS in various lesional stages

Nonlesional, Stage 0 - The arterial endothelium in the first two weeks of diet as well as that of noninvolved regions at later time intervals, by all conventional criteria appeared ultrastructurally intact. Though serum cholesterol reached values of 200-300 mg/dl (5-7 fold higher than normal), no significant changes were recorded in the cell coat moieties detectable with the probes used.

Nonlesional, Stage I - While cholesterol level was 250-500 mg/dl, and the endothelial morphology looked unchanged, cholesterol-rich extracellular phospholipid liposomes (Simionescu *et al.*, 1986), and apoprotein B (Mora *et al.*, 1986) started to accumulate in the subendothelial interstitia. The pattern of the ECS binding sites detected with our probes was in general similar to that of the zones found in stage 0. By comparison with labeling values of the normolipidemic animals, in some cases a slight decrease in CF-detectable anionic sites and an enhanced endocytosis of CF particles occurred. An increase in Con A-labelable mannosyl residues (sometimes multilayered or in small clusters) was also noticed. In animals with cholesterol levels of 250-500 mg/dl, the tracers binding on MCS was not appreciably affected.

Monocyte adhesion and diapedesis, Stage II - Starting with the third week of diet (serum cholesterol ~800 mg/dl and up), while neither the EC nor the M showed ultrastructural alterations, monocytes became focally adherent to endothelium. At the site of close contact, the tracers were commonly excluded from the apposed cell surfaces. The immediately adjacent ECS variably displayed either a continuous decoration by CF or these particles labeled small patches of an aggregate area of 68-70% of the ECS. Similar CF labeling was observed on MCS, and no consistent correlation could be established between the CF binding and the concentration of serum cholesterol. The distribution of most of the other tracers was largely unaffected, with the exception of the slightly increased Con A-detectable mannosyl residues both on EC and monocytes. It was shown that *in vitro* human monocytes have a distinctively higher affinity relative to other leukocytes for binding to human EC (Pawlowski *et al.*, 1985). In our experiments *in vivo*, we found no monocytes adhering to normal endothelium. It seems that in hypercholesterolemic animals factors other than an overall change in the cell surface charge or in some oligosaccharides, may account for monocyte adhesion to ECS and subsequent diapedesis (e.g. chemoattractants of endothelial source) (Mazzone *et al.*, 1983; Berliner *et al.*, 1984; Gerrity *et al.*, 1985; Quinn *et al.*, 1985; Terranova *et al.*, 1985), or subendothelial origin (Senior *et al.*, 1980; Hunninghake *et al.*, 1981; Gerrity *et al.*, 1985; Kunimoto and Jay, 1985), or more specific components of ECS and MCS which may be involved in the local recruitment of monocytes (Gerrity *et al.*, 1985; Schwartz *et al.*, 1985), or other factors and conditions still unrevealed. Endothelial relative structural and chemical integrity during monocyte migration is not a surprise since monocyte migration (Schwartz *et al.*, 1985) as well as granulocyte diapedesis towards a chemoattractant was found not necessarily associated with structural evidence of endothelial cell injury or augmented vascular permeability (Meyrich *et al.*, 1984). This latter aspect is however at variance with other reports (Territo *et al.*, 1984). In hypercholesterolemic rabbit, monocytes continuously enter the intima: at very high level of serum cholesterol (eighth week), some changes in ECS and MCS may become more prominent.

Lesional, Stage III - The bulging lipid-laden macrophages were often covered by markedly thin endothelial cells. ECS anionic sites were, however, only slightly decreased as compared with controls but did not differ conspicuously from nonlesional areas of the same artery. This was paralleled by an also slight reduction in FH-detectable sialyl residues, whereas the mannosyl moieties continued to be very frequent, though serum cholesterol was about 20 times higher than in controls (800-900 mg/dl). It remains to be elucidated whether the enlarging foam cells can directly affect the overlying endothelium by increased tension or by toxic products (Faggiotto *et al.*, 1984). No endothelial denudation or platelet adhesion was detected on such areas. The presence of EC enriched in WGA-binding sites occurring next to normally WGA-decorated EC, was a feature for the clarification of which additional investigations are needed. The ultrastructural similarity between these two types of EC with such a different WGA-labeling, is a good example of how a modulation remarkable biochemically is not necessarily reflected in the morphologic aspect of a cell.

Lesional, Stage IV - Endothelial cells moderately loaded with lipid inclusions maintained a fairly normal labeling pattern for all the probes used. When cells became heavily loaded with lipid deposits, looking as true 'endothelial-derived foam cells' (Lupu *et al.*, 1986), the intracellular components appeared to a degree reorganized. On such cells, while HUP-labeled cationic sites, *N*-acetyl-neuraminic acid and *N*-acetyl-glucosamine residues were found unchanged, the CF-detectable anionic sites were clustered and drastically reduced in number. A remarkable decrease in CF binding to coated pits and plasmalemmal vesicles was also obvious. Less prominent was the reduction in sialic acids and in the terminal galactosyl-, and *N*-acetyl galactosaminyl residues detected with sodium periodate/FH and GO/FH, respectively. A salient finding was the high density of Con A-labeled mannosyl moieties, and the persistance of EC enriched in WGA-binding sites observed at early stages as well. Since the decrease in CF-binding sites was much more intense than that in FH-binding sites, this suggests that the anionic sites most affected by hypercholesterolemia were the sulfated proteoglycans, and much less the sialic acids. Significant reduction in ECS sialic residues by neuraminidase treatment have been implied in the increased LDL uptake (Görög and Born, 1982). The pronounced enhancement of ECS in RCA-labeled terminal and/or subterminal galactosyl moieties and especially in the Con A-detectable mannosyl residues may represent some of the defensive responses of these cells to hypercholesterolemia.

Lesional, Stage V - The endothelium surrounding the site of a foam cell egress from the intima, exhibited two continuous regions distinctly labeled by some of the probes. The luminal surface displayed a variable density of CF-binding sites ranging from normal to a ~50% reduction, the former being most frequently encountered. On some areas, the cationic groups, sialyl residues and subterminal galactosyl moieties were usually at control levels. The junctional surface however as well as the opposed MCS were scarcely decorated by CF and RCA/LacN-BSA-Au probes, indicating that at the cell to cell contact in this process a conspicuous simplification in the chemical constituents of both ECS and MCS may take place. Other alternative

explanations may be also considered. The junction in this stage is permeated by CF, as well as by lipoproteins (Mora *et al.*, 1986) and albumin (Simionescu *et al.*, manuscript in preparation).

Onset and progression of changes in ECS components

The HUP-labeled cationic groups seemed virtually unchanged during the 8 week hypercholesterolemia; some more minute modulations could be however not visible due to the peroxidatic amplification effect on the actual location of the reaction product.

As compared with the nonlesional areas, the CF-detectable anionic groups became significantly diminished only on heavily lipid-laden endothelial cells (stage IV). The CF decoration of EC plasma membrane was only slightly lower in hyperlipidemic relative to normolipidemic rabbit. These modulations were paralleled at even lower values by FH and GO/FH labeling.

The residues marked by WGA/M-Au (*N*-acetyl-neuraminic acid and *N*-acetyl-glucosamine) remained largely unaltered with the exception of the EC enriched in WGA-binding sites (not found in normolipidemic rabbit), which persisted and apparently increased in number as the diet progressed.

Mannosyl residues as detected by Con A/HRP-Au were rapidly increased by hypercholesterolemia, and this unexpected response was continuously enhanced towards the eighth week of diet.

Both terminal and subterminal galactosyl residues as well as *N*-acetyl-galactosaminyl moieties revealed by GO/FH and RCA/LacN-BSA-Au, respectively, appeared to be very little modified by the very high levels of serum cholesterol or by the underlying intimal lesions.

All together, EC and ECS of aorta, coronary and vena cava, seemed to be not much altered even by very high concentrations of serum cholesterol. Changes or local variations in the chemistry and charge of ECS and MCS appeared only after extracellular and intracellular accumulation of lipoprotein-derived material and stromal reaction into the arterial intima. Even in areas of fatty streak formation, the only EC with marked cell surface alterations were those transforming into lipid-laden cells. These represent a minority in a lesional area. The remarkable resistance of EC and ECS to high levels of hypercholesterolemia was also observed in hamsters at 10 or 11 weeks of diet (serum cholesterol = 1,140-1,500 mg/dl) when CF labeling was quasinormal even on lesional regions (Nistor A., manuscript in preparation).

These results suggest that in the lesion-prone regions of arterial intima in hypercholesterolemic rabbit, during the prelesional stages (before monocyte adherence, migration and foam cell formation), the intimal lipid accumulation is not preceded by significant changes in ECS and MCS charge and in the glycoconjugates detected by our probes. The lesions so far detectable started in subendothelium by accumulation of a lipoprotein-derived material: subsequently, the local reaction involves progressively the extracellular matrix, macrophages and smooth muscle cells. When EC became loaded with lipid deposits and possibly inflicted by the progressing subendothelial lesion, their cell surface showed important changes in the acidic groups and negative charge while preserving unchanged other moieties. Even at very high concentrations of serum cholesterol (up to 2,000 mg/dl = ~50 fold higher than normal), although the anionic sites on both ECS and MCS were markedly reduced, the process of monocyte migration into, and foam cell egress from the intima still continues, probably as a clearing mechanism of the diseased vessel wall.

ACKNOWLEDGMENTS

We thank R. Mora and E. Vasile for data on plasma lipid analysis and A. Hillebrand and A. Nistor for monitoring the experimental model. We gratefully acknowledge the excellent technical assistance of V. Craciun, M. Toader, E.P.Georgescu (surgery and biochemistry), M. Misici (ultramicrotomy), G.V. Ionescu, E. Stefan, M. Raicu (photography), C. Neacsu (graphic work) and D. Neacsu and A. Azamfirei (editing and typing).

Preliminary findings of this work were presented at the Workshop on 'Cellular and Molecular Events in Atherogenesis', Bucharest, Romania, May 13-16, 1985, Abstract Volume, pp. 14, 18, 33.

Supported by the Ministry of Education, Romania, and by the National Institutes of Health Grant HL-26343.

REFERENCES

Berliner J.A., Territo M. and Fogelman A.M., 1984. Monocyte chemotactic factor produced by large vessel endothelial cells. *Arteriosclerosis*, **4**, 524a.

Faggiotto A. and Ross R., 1984. Studies of hypercholesterolemia. II. Fatty streak conversion to fibrous plaque. *Arteriosclerosis*, **4**, 341-356.

Faggiotto A., Ross R. and Harker L., 1984. Studies of hypercholesterolemia in the nonhuman primate. I. Changes that lead to fatty streak formation. *Arteriosclerosis*, **4**, 323-340.

Gerrity R.G., 1981. The role of the monocyte in atherogenesis. I. Transition of blood-born monocytes into foam cells in fatty lesions. *Am. J. Pathol.*, **103**, 181-190.

Gerrity R.G., Richardson M., Somer J.B., Bell F.P. and Schwartz C.J., 1977. Endothelial cell morphology in areas in vivo Evans blue uptake in the aorta of young pigs. II. Ultrastructure of the intima in areas of differing permeability to proteins. *Am. J. Pathol.*, **89**, 313-334.

Gerrity R.G., Gass J.A. and Soby L., 1985. Control of monocyte recruitment by chemotactic factor(s) in lesion-prone areas of swine aorta. *Arteriosclerosis*, **5**, 55-66.

Goldstein J.L., Ho Y.K., Brown M.S., Innerarity T.L. and Mahley R.W., 1980. Cholesteryl ester accumulation in macrophages resulting from receptor-mediated uptake and degradation of hypercholesterolemic canine β-very low density lipoproteins. *J. Biol. Chem.*, **255**, 1839-1848.

Görög P. and Born G.V.R., 1982. Increased uptake of circulating low-density lipoproteins and fibrinogen by arterial walls after removal of sialic acid from their endothelial surface. *Br. J. Exp. Pathol.*, **63**, 447-451.

Hanson G., Biornheden T., Bylock and Bondjers G., 1981. Fc dependent binding of monocytes to areas with endothelial injury in the rabbit aorta. *Exp. Mol. Pathol.*, **34**, 264-280.

Hunninghake G.W., Davidson J.M., Rennard S., Szapiel S., Gadek J.E. and Crystal R.G., 1981. Elastin fragments attract macrophage precursors to diseased sites in pulmonary emphysema. *Science*, **66**, 925-927.

Joris I., Zand T., Nunnari J.J., Krolikowski F.J. and Majno G., 1983. Studies on the pathogenesis of atherosclerosis. I. Adhesion and emigration of mononuclear cells in the aorta of hypercholesterolemic rats *Am. J. Pathol.*, **113**, 341-358.

Joris I., Billingham M.E. and Majno G., 1984. Human coronary arteries. An ultrastructural search for the early changes of atherosclerosis. *Fed. Proc.*, **43**, 710a.

Kunitomo M. and Jay M., 1985. Elastin fragment-induced monocyte chemotaxis. The role of desmosines. *Inflammation*, **9**, 183-188.

Lfabu M., Ghinea N., Muresan V., Colcfag J., Hasu M. and Simionescu N., 1987. Cell surface chemistry of arterial endothelium and blood monocytes in the normolipidemic rabbit. *J. Submicrosc. Cytol.*, **19**, 193-208.

Lewis J.C., Taylor R.G., Jones N.D., St Clair R.W. and Cornhill J.F., 1982. Endothelial surface characteristics in pigeon coronary artery atherosclerosis. I. Cellular alterations during the initial stages of dietary cholesterol challenge. *Lab. Invest.*, **46**, 123-138.

Lupu F., Danaricu I. and Simionescu N., 1986. Endothelial cell-derived foam cells in experimental atherosclerosis. A physical, cytochemical and ultrastructural study. Fourth International Symposium on the Biology of the Vascular Endothelial Cell, Noordwykerhout, The Netherlands, Vol. Abstr., p. 124.

Mahley R.W., 1982. Atherogenic hyperlipoproteinemia. The cellular and molecular biology of plasma lipoproteins altered by dietary fat and cholesterol. *Med. Clin. North Am.*, **66**, 375-402.

Mahley R.W., 1983. Development of accelerated atherosclerosis. Concepts derived from cell biology and animal model studies. *Arch. Pathol. Lab. Med.*, **107**, 393-399.

Mahley R.W., Innerarity T.L., Brown M.S., Ho Y.K. and Goldstein J.L., 1980. Cholesteryl ester synthesis in macrophages: stimulation by beta-very low density lipoproteins from cholesterol fed animals of several species. *J. Lipid Res.*, **21**, 970-980.

Mazzone T., Jensen M. and Chait A., 1983. Human arterial wall secrete factors that are chemotactic for monocytes. *Proc. Natl. Acad. Sci. USA*, **80**, 5094-5097.

Meyrich B., Hoffman L.H. and Brigham K.L., 1984. Chemotaxis of granulocytes across bovine pulmonary artery intimal explants without endothelial injury. *Tissue Cell*, **16**, 1-16.

Mora R., Lupu F. and Simionescu N., 1986. Prelesional events in atherogenesis. Colocalization of apoprotein B, unesterified cholesterol, and extracellular phospholipid liposomes in lesion-prone areas of aortic intima in hyperlipidemic rabbit. *J. Cell Biol.*, (in press).

Pawlowski N.A., Abraham E.L., Pontier S., Scott W.A. and Cohn Z.A., 1985. Human monocyte-endothelial cell interaction in vitro. *Proc. Natl Acad. Sci. USA*, **82**, 8208-8212.

Quinn M.T., Parthasarathy S. and Steinberg D., 1985. Endothelial cell-derived chemotactic activity for mouse peritoneal macrophages and the effects of modified forms of low density lipoprotein. *Proc. Natl. Acad. Sci. USA*, **82**, 5949-5953.

Ross R., 1986. The pathogenesis of atherosclerosis. An update. *New. Engl. J. Med.*, **314**, 488-500.

Schwartz C.J., Spragne E.A., Kelley H.L., Valente A.J. and Suenram C.A., 1985. Aortic intimal monocyte recruitment in the normo and hypercholesterolemic baboon (Papio cynocephalus). An ultrastructural study: implications in atherogenesis. *Virchows Arch. (Pathol. Anat.)*, **405**, 175-195.

Senior R.M., Griffin G.L. and Mecham R.P., 1980. Chemotactic activity of elastin-derived peptides. *J. Clin. Invest.*, **66**, 859-862.

Simionescu M. and Simionescu N., 1986. Functions of the endothelial cell surface. *Annu. Rev. Physiol.*, **48**, 279-293.

Simionescu M., Simionescu N. and Palade G.E., 1982. Biochemically differentiated microdomains of the cell surface of capillary endothelium. *Ann. NY Acad. Sci.*, **401**, 9-24.

Simionescu N., Vasile E., Lupu F., Popescu G. and Simionescu M., 1986. Prelesional event in atherogenesis. Accumulation of extracellular cholesterol-rich liposomes in the arterial intima and cardiac valves of the hyperlipidemic rabbit. *Am. J. Pathol.*, **123**, 109-125.

Terranova V.P., Di Florio R., Lyali R.M., Hic S., Friesel R. and Maciag T., 1985. Human endothelial cells are chemotactic to endothelial cell growth factor and heparin. *J. Cell Biol.*, **101**, 2330-2334.

Territo M., Berliner J.A. and Fogelman A.E., 1984. Effect of monocyte migration on low density lipoprotein transport across aortic endothelial cell monolayers. *J. Clin. Invest.*, **74**, 2279-2284.

Weber G., Fabbrini P. and Resi L., 1973. On the presence of a Concanavalin A-reactive coat over the endothelial aortic surface and its modification during early experimental cholesterol atherogenesis in rabbits. *Virchows Arch. A (Pathol. Anat.)*, **359**, 299-307.

Weber G., Fabbrini P., Resi L., Mattei F.M. and Tanganelli P., 1984. Lack of endothelial Con A-reactivity and delayed atherosclerotic involvement of cerebral arteries in hypercholesterolemic and hypertensive New Zealand rabbits. *Arteriosclerosis*, **4**, 53a.

Wissler R.W. and Vesselinovitch D., 1968. Experimental models of human atherosclerosis. *Ann. NY Acad. Sci. USA*, **149**, 907-922.

Zlatkis A. and Zak B., 1969. Study of a new reagent. *Anal. Biochem.*, **29**, 143-148.